Heliox simulations for initial management of congenital laryngotracheal stenosis

Marine del Puppo, Lionel Meister, Marc Médale, Chloé Allary, Richard Nicollas, Eric Moreddu

Received: 24 March 2022 | Accepted: 26 September 2022

DOI: 10.1002/ppul.26189

ORIGINAL ARTICLE

WILEY

Heliox simulations for initial management of congenital laryngotracheal stenosis

Marine Del Puppo MD[1,2] | Lionel Meister PhD[2] | Marc Médale PhD[2] | Chloé Allary MD[3] | Richard Nicollas MD, PhD[1,2] | Eric Moreddu MD, PhD[1,2]

[1]Department of Pediatric Otolaryngology Head and Neck Surgery, La Timone Children's Hospital, AP-HM, Aix Marseille Université, Marseille, France

[2]Energetic Mechanics Department, Institut Universitaire des Systèmes Thermiques et Industriels, UMR 7343 CNRS, Aix Marseille Université, Marseille, France

[3]Department of Pediatric Anesthesia and Intensive Care, La Timone Children's Hospital, AP-HM, Aix Marseille Université, Marseille, France

Correspondence
Marine Del Puppo, Hôpitaux Universitaires de Marseille, Aix Marseille Université, France, 264 rue St Pierre, 13005 Marseille, France.
Email: marine.del-puppo@ap-hm.fr

Abstract

Objectives: Congenital laryngotracheal stenosis is rare, potentially severe, and difficult to manage. Heliox is a medical gas effective in obstructive airway pathologies, given its physical properties. This study aims to model the interest of Heliox in reducing the respiratory work in congenital laryngotracheal stenosis, using numerical fluid flow simulations, before considering its clinical use.

Design: This is a retrospective study, performing Computational Fluid Dynamics numerical simulations of the resistances to airflow and three types of Heliox, on 3D reconstructions from CT scans of children presenting with laryngotracheal stenosis.

Patients: Infants and children who were managed in the Pediatric ENT department of a tertiary-care center and underwent CT scanning for laryngotracheal stenosis between 2008 and 2018 were included.

Results: Fourteen models of congenital laryngotracheal stenosis were performed in children aged from 16 days to 5 years, and one model of the normal trachea in a 5-year-old child. Tightest stenosis obtained the highest airway resistances, ranging from 40 to 10 kPa/L/s (up to 800 times higher than in the normal case). Heliox enabled a decrease in pressure drops and airway resistances in all stenosis cases, correlated to increasing Helium concentration.

Conclusions: Heliox appears to reduce pressure drops and airway resistances in 3D models of laryngotracheal stenosis. It may represent a supportive treatment for laryngotracheal stenosis, while waiting for specialized care, thanks to the reduction of respiratory work.

KEYWORDS

airway resistance, CFD, children, congenital laryngotracheal stenosis, CT reconstructions, fluid mechanics, Heliox

1 | INTRODUCTION

Congenital laryngotracheal stenosis is rare anomaly that can be fatal in the most severe cases or during episodes of decompensation. Its management represents a challenge for medical teams, often unfamiliar with this pathology, and with limited, ineffective, or invasive therapeutic procedures. The etiopathogenic of this pathology is complex due to growth defects of the laryngeal or tracheal cartilage leading to a narrowing flow cross-section of the newborn's airway. Other congenital pathologies may be responsible for laryngotracheal stenoses, such as vascular malformations with extrinsic compression of the laryngotracheal tree.[1–3]

The Myer–Cotton classification[4] assesses laryngotracheal stenosis according to four stages of severity, depending on the degree of narrowing. The management varies according to this severity staging, remaining surgical in severe cases.[5] Emergency care in a referral center with pediatric ENT expertise is necessary in cases of severe congenital stenosis or acute decompensation of fixed stenosis. The pathophysiological mechanism is an increase in airway resistance, associated with a decrease in the cross-section and the length of the stenosis. Airway resistance is a witness to the effort required to obtain an efficient ventilatory flow; this effort manifests in dyspnea and respiratory distress until collapse.

In extreme cases where tracheal intubation is not possible and noninvasive ventilation is insufficient, tracheotomy or extracorporeal membrane oxygenation (ECMO) is the only therapeutic option. Unfortunately, these last two therapies come with risks. Tracheotomy in newborns is known to provide high morbi-mortality.[6,7] Numerous complications, especially neurological sequelae, have been reported for ECMO in neonatal and pediatric populations.[8–10]

New therapeutic approaches are expected to optimize the emergency management of symptomatic laryngotracheal stenosis.

Helium is a gas, first discovered in 1868 by Jansens, a French astronomer.[11] It is a colorless, odorless, tasteless, biologically inert, and nontoxic gas, even with prolonged exposure. Its applications derive from its physical properties described by Hess et al.[12] particularly its low density, which is seven times lower than nitrogen and eight times lower than oxygen. Barach mixed it with oxygen in 1934,[13,14] gave it the name of Heliox, and used it in the medical field. Since then, experimental and clinical studies demonstrated its effectiveness in obstructive airway pathologies in adults and children.[15,16]

The use of Heliox in clinical practice was described in a prospective study conducted by Berkenbosch in 2004.[17] The analysis showed a preponderant use of the mixture in pediatric compared to adult populations. Obstructive pathologies of both upper and lower airways were mentioned. The main indications were post-extubation stridor and asthma exacerbations. Borglund Hemph[18] published in 2016 a review paper on the use of Heliox in upper airway obstruction in adults. Most studies demonstrated the absence of adverse effects and clinical improvement with Heliox, particularly in severe cases. However, the author emphasized the lack of consensus regarding the use of the gas, and the lack of large-scale, controlled studies, preventing any conclusion on the efficacy and safety of Heliox in these indications.

Given the reduction of the airway resistance and the respiratory work,[13–16] Heliox could offer a practical, and noninvasive alternative to the usual means for managing laryngotracheal stenosis.

Numerical fluid flow simulations, with the advantage of being noninvasive, are increasingly used by the medical and engineering communities. The study of respiratory physiology using Computational Fluid Dynamics (CFD) software is now widely recognized.[19–22] In addition, improving imaging techniques allow the realization of more accurate three-dimensional anatomical model reconstructions.[23] Works on, for example, fluid flow in the pediatric larynx,[24] tracheas,[25] and nasal cavities,[19,20] transport, and deposition of particles during aerosol therapy,[21] and behavior of inhaled air in tracheal stenoses,[22] have led to a better understanding of some pathologies and improvement of available therapies.

This study aims to model the interest of Heliox in reducing the respiratory work in congenital laryngotracheal stenosis, using numerical fluid flow simulations, before considering its clinical use.

2 | MATERIALS AND METHODS

2.1 | Patients

This study was approved by the ethical committee of our institution (APHM PADS#2019-204).

A retrospective collection of CT scans performed in the Pediatric Imaging Department of our institution, on infants and children presenting with laryngotracheal stenosis, between November 2008 and December 2018, was performed. The CT scans were acquired using a Siemens 64-detector helical scanner in the supine position; slice thickness varied from 0.6 to 1.5 mm.

According to French law, informed consent is not required for retrospective observational studies. Images used for the simulations were anonymized before Digital Imaging in Communications and Medicine (DICOM) extraction.

Data from 23 cases of laryngotracheal stenosis of various degrees of severity in children aged from 16 days to 5 years were collected. Nine stenosis cases were excluded: eight because 3D reconstruction was impossible (presence of mucous or tracheal collapse), one because the calculation convergence failed. A CT scan of a normal trachea on a 5-year-old child was added.

Out of the final 14 cases of laryngotracheal stenosis, eight were a consequence of extrinsic vascular compressions (double aortic arch, brachiocephalic arterial compression, and right aortic arch), and six were congenital laryngotracheal stenosis, one of which was associated with esophageal atresia and two with Down syndrome. Of the 14 cases of stenosis, six were classified as grade II according to Myer–Cotton's classification,[4] and eight cases were classified as grade III, four of them being over 90% tight. Cases were filed from the least (case 1) to the most severe (case 14) in terms of the degree of narrowing (Table 1).

TABLE 1 Characteristics of the stenosis cases

Case	Age (months)	Weight (kg)	Degree of narrowing (%)
N	61	18[a]	/
1	3	5, 5[a]	54
2	6	7, 4[a]	58
3	8	6, 5	60
4	37	15, 5	61
5	8	8, 2[a]	65
6	60	10	69
7	20	11[a]	71
8	4	6[a]	80
9	1	3, 2	87
10	55	16[a]	89
11	6	7, 4[a]	91
12	7	5,3	95
13	6	8	95
14	0, 5	3, 5[a]	98

[a]Estimated weights by age when real data were not available.

2.2 | 3D reconstructions of CT scans

3D models of laryngotracheal stenosis were obtained using ITK-Snap semi-automatic image segmentation software. It uses the active contour method to build a 3D surface model from CT scan slices.[26] To virtually isolate the trachea from adjacent regions, and reconstruct its entire volume, a semi-automatic threshold-based segmentation with manual corrections was carried out following the half-maximum height method[27] and the part of interest thresholding protocol[28] and by taking repeated measurements on 20 different zones of the virtual stack.[29] A set of points is then brought to follow the contours of the zone defined by the threshold level until obtaining a surface molding of the region of interest. Roughness and pressure parameters are set to the maximum to represent the geometry of stenosis as accurately as possible, especially very tight stenosis.

Surface reconstructions were exported to the Star-CCM + CFD software (Siemens, s.d.), allowing the generation of volumetric reconstructions and fluid flow modeling.[30] 3D reconstructions for the two extreme cases, cases *N* and 14, are presented in Figure 1.

2.3 | Volume mesh

Meshing consists in spatially discretizing the computational domain. Meshing uses polyhedral cells because the upper airways have complex and irregular geometry. The spatial discretization was selected to resolve developing boundary layers, referring to earlier studies[19,22] by our group for which mesh convergence analyses were performed, with a prescribed tolerance <0.5%. It turns out that 0.2 mm resolution polyhedral mesh in bulk regions and 10 prism layers in wall boundary layers constitute a working compromise between computational times and result accuracy. After meshing, the 3D meshes feature between 1 and 1.5 million cells.

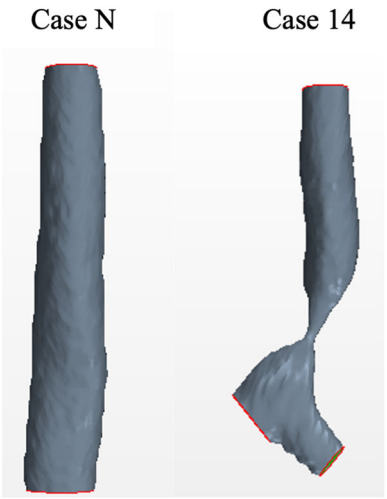

FIGURE 1 3D reconstructions from CT-scans for cases *N* and 14

TABLE 2 Gas physical properties

Gas	Density at 37°C (kg/m^3)	Dynamic viscosity (Pa.s)
Air	1.138	1.885×10^{-5}
79% N_2 + 21% O_2		
Heliox 80	0.378	2.036×10^{-5}
80% He + 20% O_2		
Heliox 70	0.488	2.047×10^{-5}
70% He + 30% O_2		
Heliox 60	0.597	2.075×10^{-5}
60% He + 40% O_2		

2.4 | Calculation parameters

Fluid was considered incompressible, the body temperature of 37°C, and values of densities and viscosities used for each gas as described by Hess[12] (Table 2).

At the entrance of the computational domain, a volume flow rate was imposed, according to the physiological resting volume flow in the function of the age and weight of each child. This volume flow rate was then converted into a mass flow rate for each gas (Table 3).

The outlet of the computational domain corresponds to the caudal section of the trachea or the two stem bronchi, depending on

TABLE 3 Mass flow rates imposed at the entrance of calculation zone for each case of stenosis and corresponding volume flow rates

Cases	Volume flow rate (L/s)	Mass flow rate (kg/s)			
		Air	H80	H70	H60
N	4.41×10^{-2}	5.02×10^{-5}	1.67×10^{-5}	2.15×10^{-5}	2.63×10^{-5}
1	3.06×10^{-2}	3.48×10^{-5}	1.16×10^{-5}	1.49×10^{-5}	1.83×10^{-5}
2	3.89×10^{-2}	4.42×10^{-5}	1.47×10^{-5}	1.9×10^{-5}	2.32×10^{-5}
3	2.97×10^{-2}	3.38×10^{-5}	1.12×10^{-5}	1.45×10^{-5}	1.78×10^{-5}
4	3.71×10^{-2}	4.22×10^{-5}	1.4×10^{-5}	1.81×10^{-5}	2.21×10^{-5}
5	3.75×10^{-2}	4.27×10^{-5}	1.42×10^{-5}	1.83×10^{-5}	2.24×10^{-5}
6	2.39×10^{-2}	2.72×10^{-5}	9.04×10^{-6}	1.17×10^{-5}	1.43×10^{-5}
7	3.21×10^{-2}	3.65×10^{-5}	1.21×10^{-5}	1.57×10^{-5}	1.92×10^{-5}
8	3.34×10^{-2}	3.8×10^{-5}	1.26×10^{-5}	1.63×10^{-5}	1.99×10^{-5}
9	1.99×10^{-2}	2.27×10^{-5}	7.53×10^{-6}	9.73×10^{-6}	1.19×10^{-5}
10	3.83×10^{-2}	4.35×10^{-5}	1.45×10^{-5}	1.87×10^{-5}	2.29×10^{-5}
11	3.89×10^{-2}	4.42×10^{-5}	1.47×10^{-5}	1.9×10^{-5}	2.32×10^{-5}
12	2.42×10^{-2}	2.76×10^{-5}	9.17×10^{-6}	1.18×10^{-5}	1.45×10^{-5}
13	4.2×10^{-2}	4.78×10^{-5}	1.59×10^{-5}	2.05×10^{-5}	2.51×10^{-5}
14	2.18×10^{-2}	2.48×10^{-5}	8.24×10^{-6}	1.06×10^{-5}	1.3×10^{-5}

the geometry of the stenosis and the 3D reconstruction, where atmospheric pressure was used as the boundary condition.

The flows were modeled according to the two regimes: without any turbulence model but with refined mesh in the boundary layer, referred to as Direct Numerical Simulations, and with turbulence modeling (κ-ω model) described by several works as suitable for tracheal airflow modeling.[21,31]

2.5 | Fluid flow configurations

We performed fluid flow computations for four gases: Air, Heliox 80, Heliox 70, and Heliox 60 (Table 2). Simulations were performed until convergence of the calculation with residual tolerance lower than 10^{-2}. We did not achieve this convergence in one case whose residual was of the order of 10^{-1}.

After the numerical simulations, we collected differential pressure between the inlet and outlet of the computational domain. This pressure drop allowed us to calculate airway resistances generated by air or Heliox for each case, according to the formula R = P/D (R for resistance, P for pressure drop, and D for volume flow rate).

3 | RESULTS

Computed pressure drops and airway resistances for each case and each gas are presented in Figure 2. The three cases with the highest resistances, ranging from 40 to 10 kPa/L/s, and the highest pressure drops correspond to the tightest stenosis (cases 12, 13, and 14), with a degree of narrowing greater than 90%. Conversely, airway resistances are minimal for case *N*, corresponding to a normal tracheal model.

In the model, the mass flow rate imposed at the entrance of the calculation zone corresponds to an identical volume flow rate for a stenosis case. Measured pressure drops decrease significantly between Air and Heliox 80 modelizations; the decrease in the pressure drops was inferior in models with a lower percentage of helium. This pattern is the same for airway resistances. The greater the rate of helium in the gas tested, the greater the decrease in pressure drops and resistances for given stenosis. The opposite effect occurs for the normal trachea case N: resistances increase when using Heliox, even with the decrease of helium concentration.

Ratios of the resistances obtained with the air simulations to those obtained with the simulations of the different Heliox concentrations are presented in Figure 3. The decrease in resistances with Heliox appears to be greater in more severe stenoses.

Results obtained with or without turbulence modeling were compared. No significant difference was found in the computed pressure losses and calculated resistances. Therefore, only pressure drops and resistances obtained without turbulence modeling are presented.

4 | DISCUSSION

CFD enabled us to show the interest of Heliox in reducing airway resistance in 3D models of laryngotracheal stenosis. In clinical practice, Heliox may be a potential alternative to the invasive

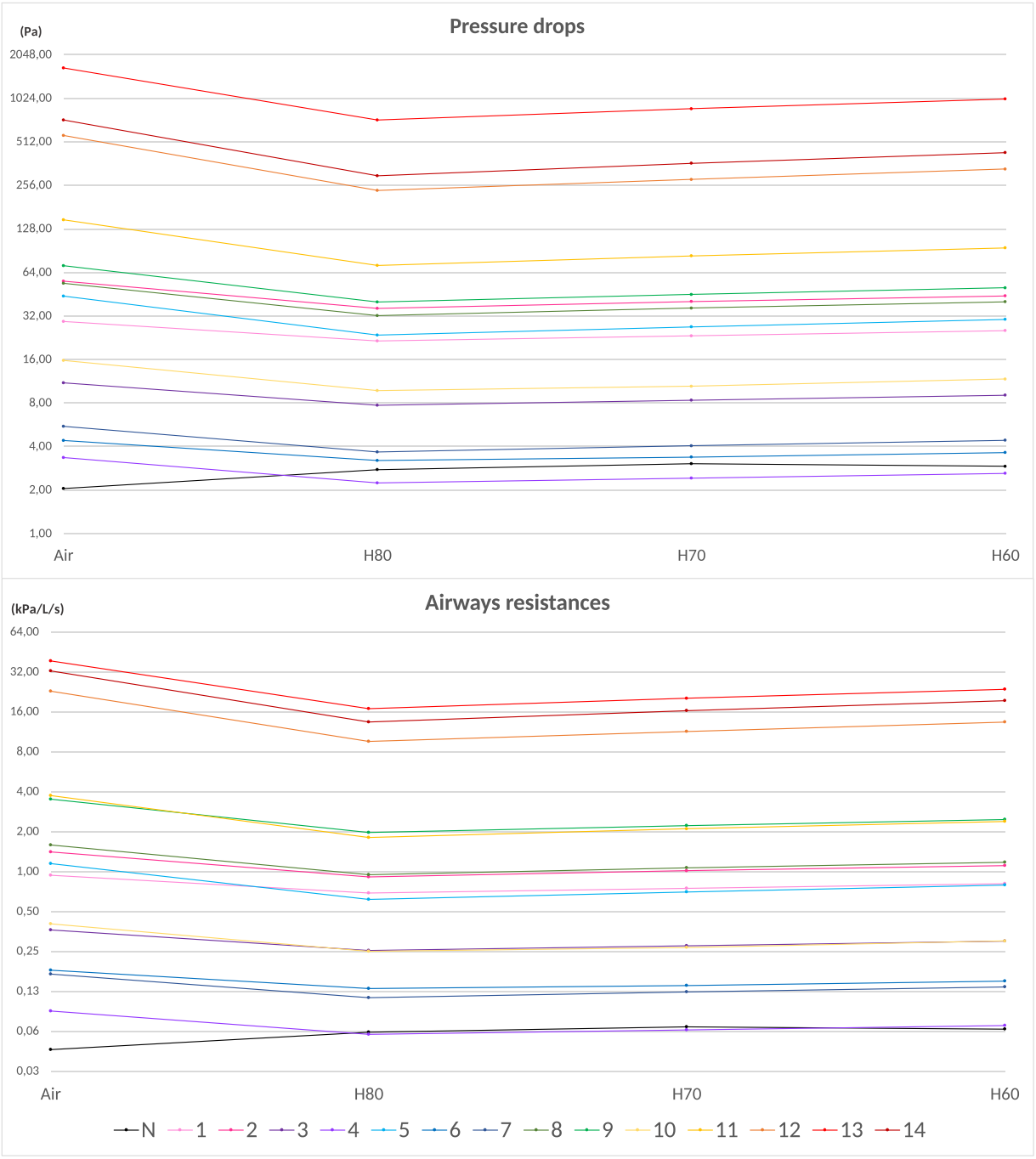

FIGURE 2 Pressure drops (in Pa) and airway resistances (in kPa/L/s) after numerical simulations, using a logarithmic scale

techniques used in the emergency management of grade II and III laryngotracheal stenosis.

These results are consistent with other experimental studies. Houck[15] explored the effect of several helium concentrations on upper airway obstructions using endotracheal tubes were used, narrowed by clamps: four degrees of narrowing and four Heliox compositions were tested. The authors found a decrease in resistance proportional to the helium concentration, especially when the stenosis is severe. Fleming[16] analyzed several respiratory parameters in healthy subjects at rest breathing through a small endotracheal tube: Heliox improved all ventilatory parameters (vital capacity, maximum expiratory volume, inspiratory flow).

Kline–Krammes[32] proposes using Heliox to transport a child with acute laryngitis to an intensive care center. This application could be interesting in the context of laryngotracheal stenosis. Their specialized care is performed in a pediatric ENT referral center, and transporting the child to this center can be risky. The use of Heliox can therefore be considered to make transport safer.

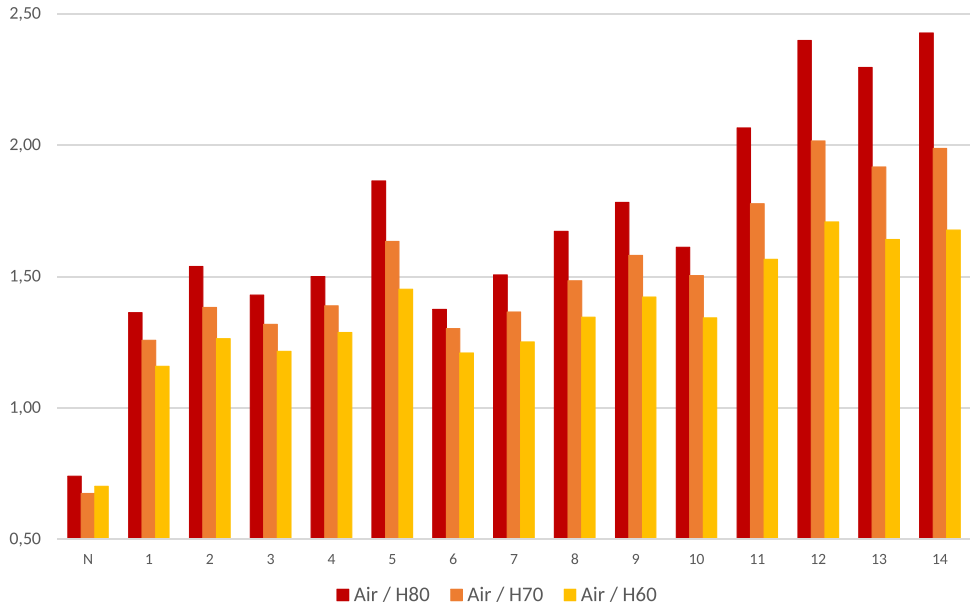

FIGURE 3 Resistance ratios (Air/Heliox) comparing air, H80, H70, and H60. In pathologic conditions, the higher is the fraction of Helium, the higher is the reduction of airway resistances.

To better understand these results, it seems essential to make some reminders of fluid dynamics.[33] Pressure drops generated during the fluid flow in a pipe depend on two components: frictional forces and variation of kinetic energy. Depending on the fluid viscosity, frictional forces are predominant in a regular pipe at a low flow rate. The pressure drop related to the variation of kinetic energy will be increased in case of sudden obstacles and high flow rate and depends then on the fluid density.

The normal case *N* corresponds to a viscous regime model, in which friction forces dominate the pressure drop. In the modelizations, volume flow rates are identical for each gas. Therefore, only intrinsic properties of the gases affect pressure drop variations and airway resistances. In case *N*, resistances increase between Air and Heliox but remain similar for all types of Heliox. In this normal case, a viscous regime prevails, and resistances increase with the viscosity, which is almost equivalent for the three types of Heliox tested but lower for air (Table 2). In all our cases of stenosis, in which the inertial regime is predominant, the decrease in airway resistance is as important as the gas' helium concentration is high, and therefore its density is low.

During the realization of our study, we elaborated two models of calculation of the mass flow rates imposed at the entrance of the calculation zone. In the first model, the flow rates were calculated so that the oxygen flow rate was identical to the one provided during air ventilation at rest. However, this way of calculating ventilation rates remains far from respiratory physiology. Respiratory control depends on several nerve centers whose mission is to ensure homeostasis, that is, maintaining constant oxygen, carbon dioxide, and pH values regardless of metabolic needs and ambient conditions.[34] Elimination of carbon dioxide is one of the significant challenges of ventilation that is not considered here. We have therefore chosen the model presented above, which seems more adapted to the simulation of respiratory ventilation. It should be remembered that the mass flow rates vary according to the tested gases, but the volume flow rate remains the same for one case, calculated according to the age and weight of each child. In other works involving flow simulations in the upper airways, the boundary conditions imposed at the entrance to the calculation zone may vary. Depending on the study's objective, pressures are sometimes set at the entry or exit of the calculation zones.[24,35] In the majority of studies,[21,22,25,36,37] a volume flow rate is selected and applied at the entrance to the calculation zone. This flow rate sometimes declines in several values to respect an extended standard deviation of ages, for example. It is often higher than a physiological flow rate in spontaneous ventilation. In our study and this model, we tried to calculate a flow rate as close as possible to the physiological flow rate of each child in spontaneous ventilation at rest. Several limitations can be found on this point. In a situation of respiratory distress, the child may be in a polypnea or even bradypnea situation, with consequent variations in respiratory flow. Moreover, these children are often taken care of by emergency medical units or intensive care units in which they will be ventilated according to a predefined flow, often higher than their respiratory flow at rest. Further modeling may be necessary at higher flow rates, similar to those used in these care settings.

Regarding other limitations of this study, the CT scan data available to perform our modeling does not allow us to consider the dynamic movements of the airways during the breathing cycle. Indeed, muscle movements mainly, but also other external forces such as gravity, impact the airways' geometry according to the ventilatory time. Recent publications[38,39] propose using ultra-short

echo time (UTE) MRI to perform a dynamic measurement of the trachea. Hysinger[38] shows the correlation between UTE MRI measurements and bronchoscopy in the evaluation of neonatal tracheomalacia. Bates[39] validates the use of this imaging technique in defining the boundary conditions necessary for dynamic CFD simulations of breathing. We do not have information on the ventilatory time (inspiration or expiration) during the acquisition of our images; this data is challenging to collect in young children whose active participation in the examination is impossible. Moreover, this study is retrospective and observative of children. CT scans were not performed for scientific research but clinical management because they have better anatomical performance than MRI for pre-surgical assessment. To limit X-ray exposure in a pediatric population, we cannot afford to increase the acquisition time of CT scans and retrospectively analyze the time of the respiratory cycle, as it could be performed with MRI, which is a nonirradiating technique. The absence of the dynamic airway dimension in our modeling requires us to moderate our conclusions about the effectiveness of Heliox on our model, and further studies are needed to validate its clinical applicability.

Results in our model suggest significant variations found in the airway resistance values in the case of laryngotracheal obstruction. Functional ventilatory exploration techniques allow the calculation of airway resistances, as the flow interruption technique.[40] This technique allows to obtain an interrupter resistance R_{int} value, reflecting the airway resistance from the mouth to the pulmonary alveoli, considering the participation of the thoracic cage, and is used mainly in obstructive pathologies of the lower airways such as asthma. This measurement is not validated in children under 3 years old. There is no technique for targeted measurement of laryngeal and tracheal resistance, and no study was found on this issue. Reference values of R_{int} range from 3 to 0.005 kPa/L/s, which seems consistent with our values found in normal *N* and loosely tight stenosis. Resistance values found in cases of tight stenosis are very high, with an increase of a factor of about 800 between case *N* and case 13. These results should be taken with caution, as no other study presenting such results and allowing a comparison has been found in the literature. Modeling in cases of extreme stenosis geometry is more likely to be unreliable, and further studies should be undertaken to validate these values.

Moreover, this study only presents a fluid flow model in laryngotracheal stenosis. It does not consider other factors that can modify ventilatory parameters and clinical response, such as bronchopulmonary dysplasia, lung damage, and nasal or pharyngeal obstruction.

In our work, the decrease in resistance with Heliox does not seem to be proportional for each case. It may be influenced by some factors, such as the geometry of laryngotracheal stenosis. Brouns[37] found in an experimental study of flow modeling in cases of tracheal stenosis that the pressure drop increases exponentially with the degree of stenosis, particularly from a 70% narrowing. Houck[15] also describes a greater interest in Heliox on experimental models of narrowed stenosis. In addition, fluid dynamics principles suggest that the geometry of the obstacle, notably the singularity or regularity of the stenosis, may influence the effectiveness of Heliox. Indeed, as we explained previously, in the case of regular flow disturbances, the pressure drop is mainly due to the friction forces of the fluid on the walls and then depends on the fluid's viscosity. Conversely, in the case of singular flow disturbances and inertial regimes, the sudden variation of kinetic energy dominates, where the density of the fluid enters into play. Thus, Heliox, given its biomechanical properties (Table 2), is likely to reduce pressure losses and airway resistance in abrupt stenosis thanks to its low density with respect to air but could be deleterious in long and regular stenosis. In most cases, the geometrical complexity of stenosis prevents the classification by a single indicator such as the degree of narrowing in Myer–Cotton Classification.[4] Indeed, two stenoses may have the same degree of narrowing but very different tortuosity, average cross-section, and so on, leading to different pressure drops. Therefore, an indicator more representative of the actual pressure drop is welcome to characterize the stenosis geometry better. Moreover, our work did not include stenosis cases with a narrowing of less than 50%. Since resistance increases during ventilation with Heliox in the normal case *N*, it could be interesting to perform flow simulations with less tight stenosis to determine from which severity grade Heliox becomes deleterious. However, the difficulty lies in obtaining CT images of less severe stenosis, as they often do not require this imaging test.

5 | CONCLUSION

Heliox allows the reduction of pressure drops and airway resistances in 3D static models of laryngotracheal stenosis classified as grade II and III in the Myers–Cotton Classification. Modeling was carried out using Computational Fluid Dynamic software. The decrease in respiratory work correlates to helium concentration in the gas. This study enables us to consider Heliox as a potentially helpful treatment of laryngotracheal stenosis in children to temporize situations in emergency cases while waiting for the necessary specialized care. Ongoing studies aim at analyzing the geometrical impact of laryngotracheal stenosis on the interest of Heliox and to validate its interest in clinical practice.

AUTHOR CONTRIBUTIONS

Marine Del Puppo participated in the investigation, formal analysis, and methodology in this study, and wrote the original draft. Lionel Meister provided resources and software; and helped with formal analysis. Marc Médale participated in the conceptualization of the study, supervision, validation, and reviewing the manuscript. Chloé Allary provided validation of the study. Richard Nicollas participated in conceptualization and methodology of this study; provided supervision and reviewing of the manuscript. Eric Moreddu provided analysis of the data, supervision, reviewing, and writing of the

manuscript. All authors discussed the results and implications and commented on the manuscript at all stages.

ACKNOWLEDGMENT

The authors would like to thank Pr Peter Bull for his helpful comments on the manuscript. No funding source supported our work.

DATA AVAILABILITY STATEMENT

The datasets analyzed during the current study are available from the corresponding author on reasonable request.

CONFLICT OF INTEREST

The authors declare no conflict of interest.

ORCID

Marine Del Puppo http://orcid.org/0000-0002-5446-5263
Richard Nicollas http://orcid.org/0000-0002-1010-575X
Eric Moreddu http://orcid.org/0000-0003-2476-9554

REFERENCES

1. Kakodkar KA, Schroeder Jr., JW, Holinger LD. Laryngeal development and anatomy. *Adv Otorhinolaryngol*. 2012;73:1-11.
2. Triglia JM, Nicollas R, Roman S. Management of subglottic stenosis in infancy and childhood. *Eur Arch Otorhinolaryngol*. 2000;257(7):382-385.
3. Nicollas R, Moreddu E, Le Treut-Gay C, Roman S, Mancini J, Triglia JM. Laryngotracheal stenosis in children and infants with neurological disorders: management and outcome. *Ann Otol Rhinol Laryngol*. 2016;125(12):1025-1028.
4. Myer CM, O'Connor DM, Cotton RT. Proposed grading system for subglottic stenosis based on endotracheal tube sizes. *Ann Otol Rhinol Laryngol*. 1994;103(4):319-323.
5. Cotton R. Management of subglottic stenosis in infancy and childhood: review of a consecutive series of cases managed by surgical reconstruction. *Ann Otol Rhinol Laryngol*. 1978;87(5):649-657.
6. Carr MM, Poje CP, Kingston L, Kielma D, Heard C. Complications in pediatric tracheostomies. *Laryngoscope*. 2001;111(11):1925-1928.
7. Corbett HJ, Mann KS, Mitra I, Jesudason EC, Losty PD, Clarke RW. Tracheostomy—a 10-year experience from a UK pediatric surgical center. *J Pediatr Surg*. 2007;42(7):1251-1254.
8. Zwischenberger JB, Nguyen TT, Upp Jr., JR, et al. Complications of neonatal extracorporeal membrane oxygenation: collective experience from the Extracorporeal Life Support Organization. *J Thorac Cardiovasc Surg*. 1994;107(3):838-849.
9. Hervey-Jumper SL, Annich GM, Yancon AR, Garton HJL, Muraszko KM, Maher CO. Neurological complications of extracorporeal membrane oxygenation in children. *J. Neurosurg. Pediatr*. 2011;7(4):338-344.
10. Brunetti MA, Gaynor JW, Retzloff LB, et al. Characteristics, risk factors, and outcomes of extracorporeal membrane oxygenation use in pediatric cardiac ICUs: a report from the Pediatric Cardiac Critical Care Consortium Registry. *Pediatr Crit Care Med*. 2018;19(6):544-552.
11. Lockyer WJS. Helium: its discovery and applications. *Nature*. 1920;105(2638):360-363.
12. Hess DR, Fink JB, Venkataraman ST, Kim IK, Myers TR, Tano BD. The history and physics of heliox. *Respir Care*. 2006;51(6):5-12.
13. Barach AL, Eckman M. The effects of inhalation of helium mixed with oxygen on the mechanics of respiration. *J. Clin. Investig*. 1936;15(1):47-61.
14. Barach AL. The use of helium in the treatment of asthma and obstructive lesions in the larynx and trachea. *Ann Intern Med*. 1935;9(6):739-765.
15. Houck JR, Keamy MF, McDonough JM. Effect of helium concentration on experimental upper airway obstruction. *Ann Otol Rhinol Laryngol*. 1990;99(7):556-561.
16. Fleming MD, Weigelt JA, Brewer V, McIntire D. Effect of helium and oxygen on airflow in a narrowed airway. *Arch Surg*. 1992;127(8):956-960.
17. Berkenbosch JW, Grueber RE, Graff GR, Tobias JD. Patterns of Helium-Oxygen (heliox) usage in the critical care environment. *J Intensive Care Med*. 2004;19(6):335-344.
18. Borglund Hemph A, Jakobsson JG. Helium–oxygen mixture for treatment in upper airway obstruction; a mini-review. *J. Acute Med*. 2016;6(4):77-81.
19. Moreddu E, Meister L, Philip-Alliez C, Triglia JM, Medale M, Nicollas R. Computational fluid dynamics in the assessment of nasal obstruction in children. *Eur. Ann. Otorhinolaryngol. Head Neck Dis*. 2019;136(2):87-92.
20. Moreddu E, Meister L, Dabadie A, Triglia JM, Médale M, Nicollas R. Numerical simulation of nasal airflows and thermal air modification in newborns. *Med Biol Eng Comput*. 2020;58(2):307-317.
21. Rahimi-Gorji M, Pourmehran O, Gorji-Bandpy M, Gorji TB. CFD simulation of airflow behavior and particle transport and deposition in different breathing conditions through the realistic model of human airways. *J Mol Liq*. 2015;209:121-133.
22. Mimouni-Benabu O, Meister L, Giordano J, et al. A preliminary study of computer assisted evaluation of congenital tracheal stenosis: a new tool for surgical decision-making. *Int J Pediatr Otorhinolaryngol*. 2012;76(11):1552-1557.
23. Mizuguchi S, Motomura Y, Maki J, et al. Tracheal size and morphology on the reconstructed CT imaging. *Pediatr Crit Care Med*. 2019;20(8):e366.
24. Nicollas R, Giordano J, Perrier P, et al. Modelling sound production from an aerodynamical model of the human newborn larynx. *Biomed Signal Process Control*. 2006;1(2):102-106.
25. Allen GM, Shortall BP, Gemci T, Corcoran TE, Chigier NA. Computational simulations of airflow in an in vitro model of the pediatric upper airways. *J Biomech Eng*. 2004;126(5):604-613.
26. Yushkevich PA, Piven J, Hazlett HC, et al. User-guided 3D active contour segmentation of anatomical structures: significantly improved efficiency and reliability. *Neuroimage*. 2006;31(3):1116-1128.
27. Spoor CF, Zonneveld FW, Macho GA. Linear measurements of cortical bone and dental enamel by computed tomography: applications and problems. *Am J Phys Anthropol*. 1993;91(4):469-484.
28. Fajardo RJ, Ryan TM, Kappelman J. Assessing the accuracy of high-resolution X-ray computed tomography of primate trabecular bone by comparisons with histological sections. *Am J Phys Anthropol*. 2002;118(1):1-10.
29. Coleman MN, Colbert MW. Technical note: CT thresholding protocols for taking measurements on three-dimensional models. *Am J Phys Anthropol*. 2007;133(1):723-725.
30. Simcenter Star-CCM+ software v. 2019.3. Engineer innovation with multiphysics computational fluid dynamics (CFD) simulation. Accessed https://www.plm.automation.siemens.com/global/en/products/simcenter/STAR-CCM.html
31. Elcner J, Lizal F, Jicha M. Comparison of turbulent models in the case of a constricted tube. *EPJ Web Conf*. 2017;143:02020.

32. Kline-Krammes S, Reed C, Giuliano Jr., JS, et al. Heliox in children with croup: a strategy to hasten improvement. *Air Med J*. 2012;31(3):131-137.
33. Nakayama Y, Boucher RF. *Introduction to fluid mechanics*. Hodder Headline Group; 1999.
34. Degano B. Physiologie respiratoire. *Pneumologie*. 2013;10(3):1-15.
35. Walenga RL, Longest PW, Sundaresan G. Creation of an in vitro biomechanical model of the trachea using rapid prototyping. *J Biomech*. 2014;47(8):1861-1868.
36. Kleinstreuer C, Zhang Z. Laminar-to-turbulent fluid-particle flows in a human airway model. *Int. J. Multiph. Flow*. 2003;29(2):271-289.
37. Brouns M, Jayaraju ST, Lacor C, et al. Tracheal stenosis: a flow dynamics study. *J Appl Physiol*. 2007;102(3):1178-1184.
38. Hysinger EB, Bates AJ, Higano NS, et al. Ultrashort echo-time MRI for the assessment of tracheomalacia in neonates. *Chest*. 2020;157(3):595-602.
39. Bates AJ, Schuh A, McConnell K, et al. A novel method to generate dynamic boundary conditions for airway CFD by mapping upper airway movement with non-rigid registration of dynamic and static MRI. *Int J Numer Methods Eng*. 2018;34(12):e3144.
40. Beydon N, Davis SD, Lombardi E, et al. An official American Thoracic Society/European Respiratory Society statement: pulmonary function testing in preschool children. *Am J Respir Crit Care Med*. 2007;175(12):1304-1345.

How to cite this article: Del Puppo M, Meister L, Médale M, Allary C, Nicollas R, Moreddu E. Heliox simulations for initial management of congenital laryngotracheal stenosis. *Pediatric Pulmonology*. 2023;58:230-238. doi:10.1002/ppul.26189